

Mitigation of Coupling in RF Tomography With Applications to Belowground Sensing

Lorenzo Lo Monte
General Dynamics
Dayton, OH USA
Lorenzo.Lomonte@gdit.com

Lee K. Patton
Air Force Research Laboratory
Dayton, OH USA
Lee.Patton@wpafb.af.mil

Michael C. Wicks
Air Force Research Laboratory
Rome, NY USA
Michael.Wicks@rl.af.mil

Abstract— In imaging applications based on RF Tomography, coupling between transmitters and receivers is a principal technical challenge to be overcome. To mitigate the coupling, we propose to activate different transmitters simultaneously, and determine their respective current source distribution in order to create electric field nulls at desired points (e.g., the receivers). The current design problem must take into consideration physical and system constraints of the radiators. As such, the current design must be formulated as a nonlinear programming problem. These constraints are discussed in details, and our method is validated using FDTD simulations.

I. INTRODUCTION

Radio frequency (RF) tomography is an imaging technique in which distributed transmitters emit narrowband low-frequency signals into the area of interest, and distributed receivers collect the scattered field from targets [1], [7]. These spatially diverse measurements are then used to form an image of the belowground scene. At low frequencies, both the transmit (Tx) and receive (Rx) radiation patterns are well represented as electrically small dipoles / loops, which afford a very accurate linear approximation to the forward scattering model [1]. As such, a plethora of inversion procedures can be used to produce images, even with subwavelength and range-independent resolution. This is true even for very large areas/volumes of interest, both in the near and the far field regions. Hitherto, RF Tomography has been considered mainly for belowground imaging of tunnels and underground facilities (UGF) [1] (see Fig. 1); however, this technique might also be applied to close-in sensing of urban environments, multistatic radar imaging, foliage penetration, building penetration, etc. [11].

Unlike wideband imaging techniques (e.g., time reversal, travel-time tomography), which are based on transmission of short pulses, RF Tomography cannot use time gating to isolate the direct path between Tx and Rx antennas [1]. Furthermore, returns from scattering bodies that are not of interest (i.e., clutter) can mask the return from weaker scatterers that are of interest. In principle, if the background field could be measured prior to the insertion of the objects of interest, then the background clutter could be subtracted [7],

[8]. However, this approach is not practical for many applications, particularly for UGF detection.

The contribution of this paper is a technique for mitigating the direct path and the strong return from known scatterers in RF tomography applications. This technique is based on multiple transmitters simultaneously emitting signals with source currents designed to create electric field nulls at receiver and clutter locations.

The paper is structured as follows. In Section II we introduce a mathematical description of the geometry used in RF Tomography. In Section III we derive the 3D forward scattering model for the case of simultaneously emitting transmitters. In Section IV, we discuss the source current design problem, which is formulated as a nonlinear optimization program. In Section V, we validate our approach using an FDTD simulation. Concluding remarks are given in Section VI.

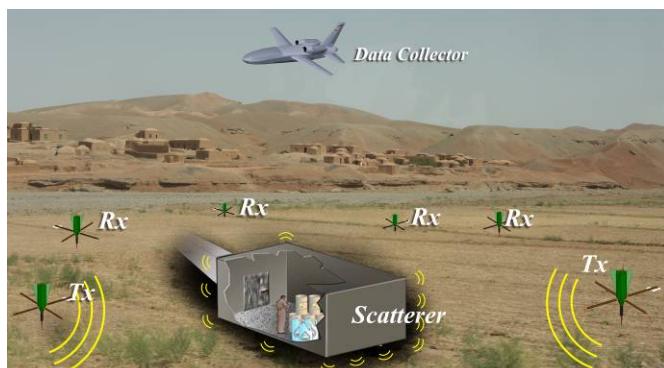


Figure 1: pictorial representation of RF Tomography for close-in sensing of underground facilities.

II. OVERVIEW OF RF TOMOGRAPHY

Consider the notional 3D transmitter-receiver geometry depicted in Fig. 2. The n -th transmitter is located at position \mathbf{r}_n^a and the m -th receiver is located at position \mathbf{r}_m^b . In order to simplify the analysis, we assume that each transmitter emits a monochromatic signal with frequency f . The multi-

Report Documentation Page

Form Approved
OMB No. 0704-0188

Public reporting burden for the collection of information is estimated to average 1 hour per response, including the time for reviewing instructions, searching existing data sources, gathering and maintaining the data needed, and completing and reviewing the collection of information. Send comments regarding this burden estimate or any other aspect of this collection of information, including suggestions for reducing this burden, to Washington Headquarters Services, Directorate for Information Operations and Reports, 1215 Jefferson Davis Highway, Suite 1204, Arlington VA 22202-4302. Respondents should be aware that notwithstanding any other provision of law, no person shall be subject to a penalty for failing to comply with a collection of information if it does not display a currently valid OMB control number.

1. REPORT DATE MAY 2010		2. REPORT TYPE		3. DATES COVERED 00-00-2010 to 00-00-2010	
4. TITLE AND SUBTITLE Mitigation of Coupling in RF Tomography With Applications to Belowground Sensing				5a. CONTRACT NUMBER	
				5b. GRANT NUMBER	
				5c. PROGRAM ELEMENT NUMBER	
6. AUTHOR(S)				5d. PROJECT NUMBER	
				5e. TASK NUMBER	
				5f. WORK UNIT NUMBER	
7. PERFORMING ORGANIZATION NAME(S) AND ADDRESS(ES) Air Force Research Laboratory, Wright Patterson AFB, OH, 45433				8. PERFORMING ORGANIZATION REPORT NUMBER	
9. SPONSORING/MONITORING AGENCY NAME(S) AND ADDRESS(ES)				10. SPONSOR/MONITOR'S ACRONYM(S)	
				11. SPONSOR/MONITOR'S REPORT NUMBER(S)	
12. DISTRIBUTION/AVAILABILITY STATEMENT Approved for public release; distribution unlimited					
13. SUPPLEMENTARY NOTES See also ADM002322. Presented at the 2010 IEEE International Radar Conference (9th) Held in Arlington, Virginia on 10-14 May 2010. Sponsored in part by the Navy.					
14. ABSTRACT In imaging applications based on RF Tomography coupling between transmitters and receivers is a principal technical challenge to be overcome. To mitigate the coupling, we propose to activate different transmitters simultaneously, and determine their respective current source distribution in order to create electric field nulls at desired points (e.g., the receivers). The current design problem must take into consideration physical and system constraints of the radiators. As such, the current design must be formulated as a nonlinear programming problem. These constraints are discussed in details, and our method is validated using FDTD simulations.					
15. SUBJECT TERMS					
16. SECURITY CLASSIFICATION OF:			17. LIMITATION OF ABSTRACT	18. NUMBER OF PAGES	19a. NAME OF RESPONSIBLE PERSON
a. REPORT	b. ABSTRACT	c. THIS PAGE			
unclassified	unclassified	unclassified	Same as Report (SAR)	5	

frequency case can be derived by invoking the principle of superposition. We further simplify the analysis by assuming the air-earth interface to be flat: in principle, our approach could be extended to irregular surfaces as well.

The air semispace is modeled as free-space medium, while the ground semispace is modeled as an homogeneous medium with background relative dielectric permittivity ϵ_D , background conductivity σ_D , and magnetic permeability μ_0 . The dielectric/conducting targets (e.g., tunnels) are assumed to reside in the investigation domain D . Transmitters and receivers must reside outside the investigation domain D . A scattering body located at position \mathbf{r}' inside D is described by a deviation in the relative dielectric permittivity $\epsilon_r(\mathbf{r}')$ and the conductivity $\sigma(\mathbf{r}')$. Unlike in other geophysical applications, the detection of underground facilities does not require the discrimination between dielectric and conducting bodies. Hence, we can for convenience define a complex-valued *contrast function*:

$$V(\mathbf{r}') = \epsilon_r(\mathbf{r}') - \epsilon_D + j(\sigma(\mathbf{r}') - \sigma_D) / 2\pi f \epsilon_0, \quad (1)$$

where ϵ_0 is the dielectric permittivity of free space, and $j^2 = -1$. A scattering body at position \mathbf{r}' can be detected by estimating $V(\mathbf{r}')$ from measurements of the scattered field, and comparing its magnitude to a threshold. In the following section, we relate $V(\mathbf{r}')$ to the measurements of the scattering field.

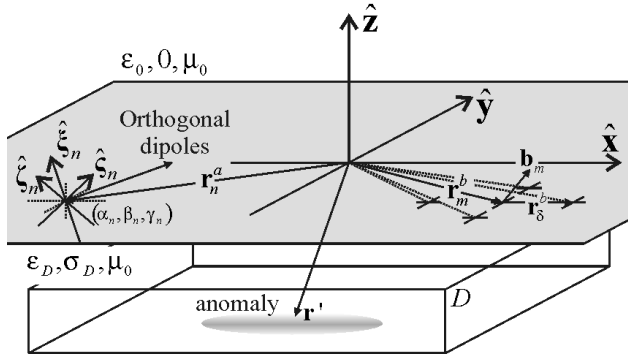


Figure 2: three dimensional geometry for the model.

III. FORWARD MODEL

To properly address the coupling problem we must account for the 3D vector nature of the electric field in the development of the forward scattering model. We assume that the n -th transmitter is constituted of (up to) three co-located but orthogonal dipole antennas. Oftentimes, the orientation of the transmitters and receivers will not be congruent with the inertial coordinate system. To account for the actual

orientation, we assume the first, second and third dipole of the n -th transmitter to be oriented along the unit vector $\hat{\zeta}_n, \hat{\xi}_n, \hat{\xi}_n$, respectively, where $\hat{\zeta}_n, \hat{\xi}_n$ and $\hat{\xi}_n$ correspond to the inertial coordinate vectors $\hat{\mathbf{x}}, \hat{\mathbf{y}}$ and $\hat{\mathbf{z}}$ rotated by α_n, β_n and γ_n , respectively. This operation can be represented by the rotation matrix \mathbf{R}_n^a , which is given by:

$$\mathbf{R}_n^a = \begin{bmatrix} \cos \gamma_n \cos \beta_n & -\sin \gamma_n \cos \beta_n & \sin \beta_n \\ \sin \gamma_n \cos \alpha_n + \cos \gamma_n \sin \beta_n \sin \alpha_n & \cos \gamma_n \cos \alpha_n - \sin \gamma_n \sin \beta_n \sin \alpha_n & -\cos \beta_n \sin \alpha_n \\ \sin \gamma_n \sin \alpha_n - \cos \gamma_n \sin \beta_n \cos \alpha_n & \cos \gamma_n \sin \alpha_n + \sin \gamma_n \sin \beta_n \cos \alpha_n & \cos \beta_n \cos \alpha_n \end{bmatrix} \quad (2)$$

Currents flowing in each orthogonal radiating dipole of the n -th transmitter can be expressed in phasor form by the vector:

$$\mathbf{d}_n = (d_{\zeta_n}^r + jd_{\zeta_n}^j) \hat{\zeta}_n + (d_{\xi_n}^r + jd_{\xi_n}^j) \hat{\xi}_n + (d_{\xi_n}^r + jd_{\xi_n}^j) \hat{\xi}_n \quad (3)$$

Clearly, from the phasor \mathbf{d}_n the current to be fed into each orthogonal radiating dipole can be computed as:

$$\begin{aligned} \mathbf{d}_n(t) &= \text{Re}(\mathbf{d}_n \exp(-j\omega t)) \\ &= \text{Re}(\mathbf{d}_n) \cos(\omega t) + \text{Im}(\mathbf{d}_n) \sin(\omega t) \quad (4) \\ &= d_{\zeta_n}^r(t) \hat{\zeta}_n + d_{\xi_n}^r(t) \hat{\xi}_n + d_{\xi_n}^r(t) \hat{\xi}_n \end{aligned}$$

$$d_{\zeta_n}^r(t) = \sqrt{(d_{\zeta_n}^r)^2 + (d_{\zeta_n}^j)^2} \sin(\omega t + \tan^{-1}(d_{\zeta_n}^r / d_{\zeta_n}^j)) \quad (5)$$

$$d_{\xi_n}^r(t) = \sqrt{(d_{\xi_n}^r)^2 + (d_{\xi_n}^j)^2} \sin(\omega t + \tan^{-1}(d_{\xi_n}^r / d_{\xi_n}^j)) \quad (6)$$

$$d_{\xi_n}^r(t) = \sqrt{(d_{\xi_n}^r)^2 + (d_{\xi_n}^j)^2} \sin(\omega t + \tan^{-1}(d_{\xi_n}^r / d_{\xi_n}^j)) \quad (7)$$

where $\omega = 2\pi f$. Clearly, any desired phasor form \mathbf{d}_n can be synthesized by driving the dipoles with the appropriate current amplitude and phase. The phasor \mathbf{d}_n , which is measured with respect to a local coordinate system, can be represented with respect to the inertial coordinate system through the transformation:

$$\mathbf{a}_n = \mathbf{R}_n^a \cdot \mathbf{d}_n \quad (8)$$

If we assume that the receiving elements are constructed in the same way as the transmitters, then we can model the m -th receive element, located at position \mathbf{r}_m^b , as measuring the received field according to the unit-norm (moment) direction $\hat{\mathbf{b}}_m$, referenced to the $(\hat{\mathbf{x}}, \hat{\mathbf{y}}, \hat{\mathbf{z}})$ coordinate system.

The field measured by the m -th receiver from the n -th transmitter was derived in [1] and [3]. In this paper, we extend this forward model by assuming that each measurement i of the electric field is function of the receiver position \mathbf{r}_m^b , receiver moment direction $\hat{\mathbf{b}}_m$, and a combination $s: \{\mathbf{r}_n^a, \forall n \in \Gamma_s\}$ of N_s transmitters simultaneously activated, represented with the index set Γ_s . The i -th field measurement is related with the contrast function according to the following equation:

$$E(i) = \mathbf{b}_m^T \cdot \sum_{n \in \Gamma_s} Q_n \mathbf{G}(\mathbf{r}_m^b, \mathbf{r}_n^a) \cdot \mathbf{a}_n + H(i) + Z + \quad (9)$$

$$k_0^2 \iiint_D V(\mathbf{r}') \mathbf{b}_m^T \cdot \mathbf{G}(\mathbf{r}_m^b, \mathbf{r}') \cdot \left[\sum_{n \in \Gamma_s} Q_n \mathbf{G}(\mathbf{r}', \mathbf{r}_n^a) \cdot \mathbf{a}_n \right] d\mathbf{r}'$$

$$k_0 = \omega \sqrt{\mu_0 \epsilon_0} \quad (10)$$

$$i = (\mathbf{r}_m^b, \mathbf{b}_m, s) \quad (11)$$

where $Q_n = j\omega\mu_0 L_n$ for a dipole of length L_n , and $Q_n = -j\omega\mu_0 A_n$ for a loop of area A_n , H represents the nonlinear term (i.e., multiple scattering) and Z represents the noise term. Matrix \mathbf{G} represents the dyadic Green's function of the problem. Expressions for free space, half-space, layered Green's Dyad are presented in [8]-[10]. Equation (9) represents the *forward model* for RF tomography using a combination s of transmitters activated at the same time. Both H and Z are assumed unknown, and represent undesired perturbations to the received scattered field. Since tunnels are static objects and the probing wavelength is large compared to the targets, we can reasonably neglect these terms, and (9) becomes a linear operator on V .

The next logical step is to collect other measurements by varying $\mathbf{r}_m^b, \mathbf{b}_m, s$ to form a measurement set:

$$\underline{E} = \{E(i)\} \quad (12)$$

Moreover, the domain D can be discretized into k voxels, each one located at \mathbf{r}'_k . Therefore, we can define the contrast vector $\underline{V} = \{V(\mathbf{r}'_k)\}$, where V_k corresponds to the contrast function evaluated at \mathbf{r}'_k . The operation of integration in (9) repeated for each i -th measurement can be discretized in a matrix \mathbf{L} operating on \underline{V} . Note that the first term in (9):

$$\mathbf{b}_m^T \cdot \sum_{n \in \Gamma_s} Q_n \mathbf{G}(\mathbf{r}_m^b, \mathbf{r}_n^a) \cdot \mathbf{a}_n \quad (13)$$

represents the coupling between a combination s of transmitters and the m -th receiver. This can also be expressed using a vector \underline{P} (see [1] for details). Therefore, the forward model can be approximated in discrete form by [1]:

$$\underline{E} \cong \mathbf{L} \underline{V} + \underline{P}. \quad (14)$$

In principle the estimation of \underline{V} can be performed as follows:

$$\hat{\underline{V}} \cong \mathbf{L}^{-1} (\underline{E} - \underline{P}) \quad (15)$$

where \mathbf{L}^{-1} can be computed using Tikhonov Regularization, Truncated SVD, Backpropagation, etc. (see [1], [2]). However, in real cases, one should expect some uncertainties in \mathbf{G} , \mathbf{r}_n^a , \mathbf{r}_m^b , \mathbf{b}_m and \mathbf{R}_n^a ; as such, once can only *estimate* the coupling effect via the vector $\hat{\underline{P}}$ and form the image using the following inversion procedure:

$$\hat{\underline{V}} \cong \mathbf{L}^{-1} (\underline{E} - \hat{\underline{P}}) \quad (16)$$

Unfortunately, each i -th entry of \underline{P} can be up to 50-60 dB higher in value than the scattering terms in the i -th entry of \underline{E} . As such, slight deviations $\underline{P} - \hat{\underline{P}}$ can be still higher than the scattering signals, and further mitigation is required. A way to overcome this problem is to dramatically reduce the magnitude of \underline{P} in order to have the deviation vector $\underline{P} - \hat{\underline{P}}$ comparable with the magnitude of \underline{E}^S . The reduction of \underline{P} can be achieved by a proper selection of the amplitude and phase of each radiating element, which is the subject of next Section.

IV. SYSTEM DESIGN

The method we propose is to design the transmit currents in each dipole of each antenna such that the direct-path signals are heavily reduced at the receiver side. This design process must be repeated for each i -th measurement. In order to provide robustness to uncertainties, we seek current distributions that produce low coupling over a small area surrounding the m -th receiver. This task is accomplished by considering a suitable set of Δ points in the neighbor of \mathbf{r}_m^b , each one positioned at a (small) distance \mathbf{r}_δ^b from \mathbf{r}_m^b (see Fig. 2). Furthermore, we can allocate a relative importance at each point by assigning each point with a weight w_δ .

The power of the coupling effect at the receiver position \mathbf{r}_m^b and moment direction \mathbf{b}_m , and in its surrounding Δ points \mathbf{r}_δ^b can be quantified via the functional:

$$J(\mathbf{a}_n) \triangleq \sum_{\delta=1}^{\Delta} w_\delta \left\| \sum_{n \in \Gamma_s} \mathbf{b}_m^T \cdot \mathcal{Q}_n \mathbf{G}(\mathbf{r}_m^b + \mathbf{r}_\delta^b, \mathbf{r}_n^a) \cdot \mathbf{a}_n \right\|_2^2, \quad (17)$$

By expanding (17) and using (8) we obtain:

$$J(\mathbf{d}_n) = \sum_{n,l \in \Gamma_s} \mathbf{d}_n^H \cdot (\mathbf{R}_n^H)^H \cdot \tilde{\mathbf{G}}_n^H \cdot \mathbf{B}_m \cdot \tilde{\mathbf{G}}_l \cdot \mathbf{R}_l \cdot \mathbf{d}_l \quad (18)$$

$$\tilde{\mathbf{G}}_{n,l} = \sum_{\delta=1}^{\Delta} w_\delta \mathcal{Q}_n \mathbf{G}(\mathbf{r}_m^b + \mathbf{r}_\delta^b, \mathbf{r}_{n,l}^a) \quad (19)$$

$$\mathbf{B}_m = (\mathbf{b}_m \cdot \mathbf{b}_m^T) \quad (20)$$

If the coupling needs to be minimized independently from the moment direction \mathbf{b}_m , then $\mathbf{B}_m = \mathbf{I}_{3 \times 3}$.

Clearly, the functional in (18) can be recast in matrix form:

$$J(\mathbf{d}_n) = \mathbf{d}^H \cdot \mathbf{K} \cdot \mathbf{d} \quad (21)$$

Where the positive semidefinite matrix \mathbf{K} is defined by

$$\mathbf{K} \triangleq \begin{bmatrix} \mathbf{R}_1^H \tilde{\mathbf{G}}_1^H \mathbf{B} \tilde{\mathbf{G}}_1 \mathbf{R}_1 & \cdots & \mathbf{R}_1^H \tilde{\mathbf{G}}_1^H \mathbf{B} \tilde{\mathbf{G}}_N \mathbf{R}_N \\ \vdots & \ddots & \vdots \\ \mathbf{R}_N^H \tilde{\mathbf{G}}_N^H \mathbf{B} \tilde{\mathbf{G}}_1 \mathbf{R}_1 & \cdots & \mathbf{R}_N^H \tilde{\mathbf{G}}_N^H \mathbf{B} \tilde{\mathbf{G}}_N \mathbf{R}_N \end{bmatrix} \succeq 0 \quad (22)$$

and \mathbf{d} represents a vector comprised of the design currents in the local coordinate systems.

$$\mathbf{d} \triangleq [\mathbf{d}_1 \quad \cdots \quad \mathbf{d}_N]^T \quad (23)$$

The optimal choice of the transmitters currents \mathbf{d}_{opt} is the vector that minimizes J . To avoid the trivial solution, we constrain the total transmitted power to be some positive scalar. Since \mathbf{d}_{opt} is invariant with respect to the choice of the power, we choose the unity for convenience.

$$\mathbf{d}_{opt} = \arg \min [J(\mathbf{d}_n)] \quad (24)$$

$$\text{subject to: } \mathbf{d}^H \cdot \mathbf{d} = 1 \quad (25)$$

The minimization of (21) using the constraint (25) can be obtained analytically using the Lagrangian multiplier method. The Lagrangian is given by

$$\Lambda = \mathbf{d}^H \cdot \mathbf{K} \cdot \mathbf{d} - \lambda (\mathbf{d}^H \cdot \mathbf{d} - 1) \quad (26)$$

Imposing $\nabla \Lambda = 0$, we obtain:

$$\mathbf{K} \cdot \mathbf{d} = \lambda \mathbf{d} \quad (27)$$

Thus, \mathbf{d}_{opt} is any eigenvector corresponding to the smallest eigenvalue of \mathbf{K} .

However, we also wish to maximize the signal-to-noise ration of the scattered signals, and this will generally occur only when each transmitter is radiating at its maximum power. As such, we prefer to solve the constrained optimization problem given by

$$\mathbf{d}_{opt} = \arg \min [J(\mathbf{d}_n)] \quad (28)$$

$$\text{subject to: } \|\mathbf{d}_n\|_2^2 = \mathbf{d}_n^H \cdot \mathbf{d}_n = 1 \quad \forall n \quad (29)$$

This power constraint represents a non-convex set of constraints, and the minimization can be performed using standard techniques such as sequential quadratic programming (SQP), or interior point methods (IP).

In practical cases, transmitters may be constructed using only two co-located orthogonal dipole (i.e., crossed dipoles), or even a single dipole. There are number of ways to handle these conditions. In this work, we simply impose the condition

$$d_{\xi_n} = 0 \quad (30)$$

when the n -th transmitter is a crossed dipole, and

$$d_{\zeta_n} = 0, \quad d_{\xi_n} = 0 \quad (31)$$

when the n -th transmitter is a single dipole.

V. SIMULATIONS

In order to demonstrate the validity of our approach, we simulated the imaging of belowground void structures representing an underground facility using close-in sensing.

The parameter of interest are $f = 5$ MHz, $\epsilon_D = 9$, and $\sigma_D = 5 \times 10^{-4}$ [S/m]. The underground facility is simulated using two cylinders of radius 1m places 10m beneath the ground (see Fig. 4).

The sensors were modeled as six transceivers (i.e., co-located transmitter and receiver) encircling the investigation

domain D (see Fig. 4). All transmitters are considered to be crossed dipoles, each one radiating at its maximum allowed power. The first dipole of each transceiver is oriented along $\hat{\mathbf{x}}$, while the second dipole is oriented along $\hat{\mathbf{y}}$, so that \mathbf{R}_n^a simplifies.

We computed the power set of the set of all transmitters and for each subset (i.e., combination s of transmitters) we optimized design currents for each receiver. Among all possible combinations, we selected only 10 measurements that provide the best coupling suppression at a particular receiver, and at 4 equally distant points ($|\mathbf{r}_\delta^b| = 0.5$ [m]) from the receiver.

The optimization was performed using the interior point algorithm [4] in the MATLAB optimization toolbox. The algorithm was initialized with a feasible point, and converged in tenths of seconds for each design. The optimization process was able to produce current designs that put nulls in excess of 50dB at the receiver locations (one such design is shown in Fig. 5).

For each combination s and Rx pair, the optimized currents were inserted into the FDTD simulator GPRMAX [6] and the forward scattered field at the surface is calculated. The field is then collected from a dual polarized receiver. In total, 120 samples are collected and inserted into (14). The corresponding underdetermined matrix equation is solved using Truncated SVD [1], and the contrast function was estimated. The resulting image is shown in Fig. 6.

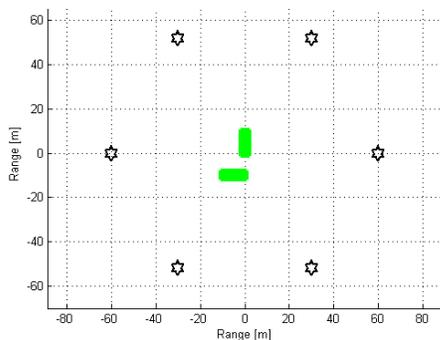


Figure 4: Simulation: Tx and Rx reside in the same region. Two tunnels (in green) are located 10m belowground.

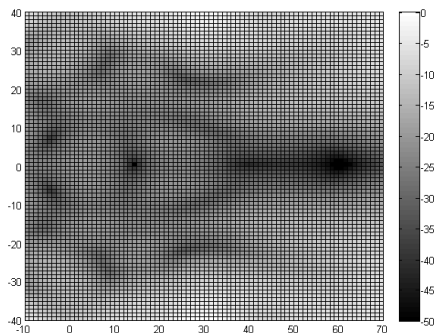


Figure 5: Snapshot of the incident electric field at the surface. The receiver located at $(-60, 0, 0)$ is experiencing a coupling below 50dB from the peak value in the domain D .

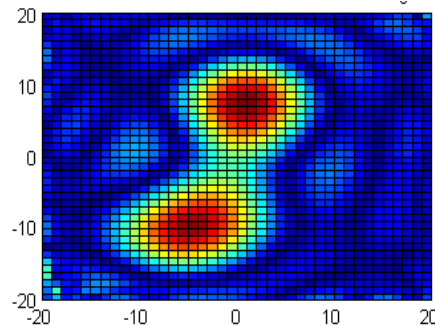


Figure 6: Reconstructed image using 120 samples and Truncated SVD. Depth slice of 10m.

VI. CONCLUSIONS

Figure 7 shows the reconstructed image of the underground scene. Using interferometric RF tomography, samples were collected *without* the need of knowing the background incident field at the receivers, since the coupling was mitigated *a priori*. Clearly, this strategy represents an important step toward a practical implementation of RF tomography for real-world belowground imaging.

VII. ACKNOWLEDGEMENT

The authors are thankful to Mr. William J. Baldygo, Air Force Research Laboratory / Sensors Directorate, for sponsoring and funding this research. We are also grateful to Prof. Margaret Cheney, Prof. Birsen Yazici, and Dr. Venky Krishnan, Rensselaer Polytechnic Institute, for their helpful suggestions and technical discussions.

REFERENCES

- [1] L. Lo Monte, D. Erricolo, F. Soldovieri, M. C. Wicks, "Radio Frequency Tomography for Tunnel Detection", *IEEE Trans. Geosci. Remote Sens.*, in press.
- [2] M. S. Zhdanov, *Geophysical Inverse Theory and Regularization Problems*, Methods in Geochemistry and Geophysics, Vol. 36, Elsevier, Amsterdam, 2002.
- [3] T. J. Cui, and W. C. Chew, "Diffraction Tomographic Algorithm for the Detection of Three-Dimensional Objects Buried in a Lossy Half-Space," *IEEE Trans. Antennas Propag.*, Vol. 50, No. 1, pp. 42-49, Jan. 2002.
- [4] A. Ruszczynski, *Nonlinear Optimization*, Princeton University Press, Princeton, NJ, 2006.
- [5] P. Meincke, "Linear GPR Inversion for Lossy Soil and a Planar Air-Soil Interface," *IEEE Trans. Geosci. Remote Sens.*, Vol. 39, No. 12, pp. 2713-2721, Dec. 2001.
- [6] A. Giannopoulos, *GPRMAX Simulator*, www.gprmax.org
- [7] J. Norgard, M. C. Wicks, and A. Drozd, "Distributed/Embedded Sub-Surface Sensors for Imaging Buried Objects with Reduced Mutual Coupling and Suppressed Electromagnetic Emissions," *Proc. International Conference on Electromagnetics in Advanced Applications (ICEAA)*, pp. 427-430, Turin, Sept. 17-21, 2007.
- [8] W. C. Chew, *Waves and Fields in Inhomogeneous Media*, IEEE Press, Piscataway NJ, 1995.
- [9] C. T. Tai, *Dyadic Green Functions in Electromagnetic Theory, Second Edition*, IEEE Press, Piscataway, NJ, 1993.
- [10] R. W. P. King, M. Owens, and T. T. Wu, *Lateral Electromagnetic Waves*. Springer-Verlag, New York, NY, 1992.
- [11] J.T. Parker, J. Norgard, "Autofocusing for RF Tomography using particle swarm optimization," *IEEE Proc. Radarcon 2008*, pp. 1-6, Rome, Italy 26-30 May 2008.